ICONHIC2026
4th International Conference on Natural Hazards & Infrastructure
29 June – 2 July 2026, Chania, Greece

On the practical conversion of fragility functions to alternative and non-spectral intensity measures

Davit Shahnazaryan*, Volkan Ozsarac, Gerard J. O'Reilly
Centre for Training and Research on Reduction of Seismic Risk (ROSE Centre), Scuola Universitaria Superiore IUSS di Pavia, Pavia 27100, Italy

ABSTRACT

This study presents a comprehensive framework for converting seismic fragility functions (FFs) between different intensity measures (IMs) using probabilistic seismic hazard analysis (PSHA) disaggregation information. The proposed methodology incorporates ground motion models directly into the conversion procedures, extending applicability beyond traditional spectral acceleration-based IMs to include non-spectral acceleration IMs. A computational tool was developed to facilitate conversions using various correlation models.

To validate the conversion approach, multiple-stripe analysis (MSA) was performed on several single-degree-of-freedom (SDOF) systems using hazard-consistent ground motion records obtained through conditional selection. The conversion strategy was extended and tested for vulnerability model conversion, addressing a gap in the literature. Various total probability-based approaches were applied in a case study, incorporating different levels of hazard information. A critical finding is that conversions from sub-optimal intensity measures such as peak ground acceleration do not enhance predictive performance when mapped to more optimal alternatives. Using converted fragility functions and a predefined consequence model, vulnerability curves were estimated to enable comprehensive comparison across exact and approximate conversion approaches. The framework effectively preserves probabilistic characteristics across different intensity measure representations while providing practitioners with a practical tool for seismic risk assessment when direct fragility functions for desired intensity measures are unavailable and structural analysis is not an option. Accompanying tools and guidance support analysts in implementing and validating these methods for their own models.

Keywords: intensity measure conversion, fragility functions, vulnerability modelling, seismic risk

INTRODUCTION

Seismic risk assessment relies on fragility and vulnerability models that probabilistically relate structural damage and economic losses to ground motion intensity. These models employ various intensity measures (IM)s depending on building typology, application purpose, and data availability. Suitability of IMs can be assessed using several criteria, typically described as sufficiency, efficiency, practicality, and unbiased-ness. Since typology-specific studies typically produce incompatible function definitions with different IMs, portfolio level risk analysis becomes problematic. While independent assets can be evaluated separately using IM-specific ground motion fields (GMF)s, correlated assets require simultaneous generation of cross-correlated fields for each IM,

* Corresponding author: Davit Shahnazaryan, Centre for Training and Research on Reduction of SeismicRisk (ROSE Centre), Scuola Universitaria Superiore IUSS di Pavia, Piazza della Vittoria 15, Pavia 27100, Italy. Email: davit.shahnazaryan@iusspavia.it

which is a computationally prohibitive task for which appropriate models are rarely if ever available (Monteiro & O'Reilly, 2026). This limitation is especially critical for interconnected systems such as infrastructure networks or building clusters where spatial dependencies exist (Abarca et al., 2022, 2025; Esposito et al., 2015; Franchin & Cavalieri, 2015; Heresi & Miranda, 2022; Mejia & O'Reilly, 2026).

As seen, regional seismic risk assessment confronts a fundamental challenge: fragility and vulnerability models from diverse sources employing incompatible IM definitions. While standardised IMs such as peak ground acceleration (PGA) or even spectral acceleration (SA) enable efficient single GMF simulations, they compromise model accuracy relative to structure or application-specific alternatives optimised for particular typologies. Advanced IMs including average spectral acceleration (Sa_{avg}) (Eads et al., 2015; Kazantzi & Vamvatsikos, 2015) and filtered incremental velocity ($FIV3(T)$) (Dávalos & Miranda, 2019), among others demonstrate improved predictive performance and explanatory power, yet remain underutilised at regional scales due to limited model availability and computation constraints.

Risk modelers frequently encounter extensive libraries of fragility and vulnerability models developed by individual research groups, each tailored to specific building typologies and employing different IM definitions. Unless systematic vulnerability model development is undertaken collectively across diverse taxonomies, practitioners cannot readily benefit from these specialised models while maintaining analytical consistency. The inability to segregate analyses and perform independent evaluations for different asset categories compels risk modelers to select among three strategic approaches. The first standardises all models to a single IM, sacrificing accuracy for computational simplicity. The second leverages multiple optimised measures through simultaneous cross-correlated GMF generation, offering improved performance but imposing severe computational demands and requiring seldom available and difficult to generate cross-correlation models (Monteiro & O'Reilly, 2026). Finally, the third strategy aims to convert existing models from diverse sources to a unified generalised IM, enabling efficient single GMF simulations while potentially allowing departure from conventional IM definitions (such as PGA). This paper concentrates on the latter strategy and examines the conversion methodology in detail, addressing source hazard information requirements, exploring advanced IMs as alternatives, and extending the methodology towards vulnerability modelling. The proposed method is trialled with several case study applications, with practical and computational tools provided, to enable analysts to perform such conversions systematically.

EXISTING CONVERSION METHODS

Various methods have been used to compare and convert fragility contributions. Early scaling approaches, such as Silva et al. (2014) and O'Reilly & Calvi (2020), adjusted median values assuming uniform hazard equivalence, neglecting variability between intensity measures (IMs). Risk-consistent conversion methods, developed by Bradley (2012) and Lin et al. (2013), overcome these limitations by preserving the mean annual frequency of exceeding a damage state across IMs, ensuring efficiency, sufficiency, and unbiasedness, and enabling more accurate fragility function conversion.

In contrast to the previous approaches relying on simplified assumptions, total probability-based conversion methods offer greater rigor by accounting for conditional relationships between IMs. Equation (1) represents the total probability theorem within the context of fragility function conversion:

$$P\,DS|\,IM\square 2\square\square = \int IM\square 1\square\square\square P\,DS|\,IM\square 1\square\square\, f\square\, IM\square 1\square|\,IM$$ (1)

where $P[DS|IM_1]$ is the original fragility function based on IM_1 and $f_{IM1|IM2}$ is the conditional distribution of IM_1 given IM_2 to result in the converted fragility function $P[DS|IM_2]$. This framework, was initially proposed by Michel (2018) and subsequently refined by Suzuki and Iervolino (2020). Their extension incorporates rupture-specific parameters such as magnitude and distance, recognising their influence on IM correlations (Equation (2)).

$$P\,DS|\,IM\square 2\square\square = \int IM\square 1\square\square\square \int M\square\square \int R\square\square P\,DS|\,IM\square 1\square, M, R\square\, f\square\, IM\square 1\square, M, R|\,IM\square 2\square\square d\,I$$ (2)

where the conditional distribution term $f_{IM1,M,R|IM2}$ was rearranged to a more familiar format of:

$$f\square\, IM\square 1\square, M, R|\,IM\square 2\square\square = f\square\, IM\square 1\square|\,IM\square 2\square M, R\square\, f\square M, R|\,IM\square 2\square\square$$ (3)

where $f_{IM1|IM2,M,R}$ is the conditional distribution of IM_1 given IM_2 and the rupture parameters M and R. This conditional distribution is widely used in the conditional spectrum (CS) and generalised conditional intensity measure (GCIM) ground motion selection approaches (Bradley, 2010; Lin et al., 2013). The $f_{M,R|IM2}$ term is computed using the disaggregation of the PSHA results for IM_2 in terms of M and R. Suzuki and Iervolino (2020) noted that this strictly refers to the occurrence of $IM_2=im_2$ and not its exceedance $IM_2>im_2$ as is typically done. Fox et al. (2016) provides further information on the implications of either approach.

PROPOSED CONVERSION METHOD

This paper further extends the probability-based framework by incorporating all scenario parameters, denoted as *Rup* (e.g., soil condition, rake, hypo-central depth), together with ground motion models (GMM)s, into the conversion equation:

$$P\,DS|\,IM\square 2\square\square = \int IM\square 1\square\square\square \int Rup\square\square P\,DS|\,IM\square 1\square\square\, f\square\, IM\square 1\square|\,IM\square 2\square, Rup\square\, f\square Rup|\,IM$$ (4)

The proposed methodology within this paper leverages the complete disaggregation output format of the OpenQuake engine (Pagani et al., 2014), where instead of using basic information on the relative contributions of only M and R to the hazard, all rupture scenario parameters and associated GMMs are used. this necessitates computing the rupture disaggregation for the target IM and establishing conditional distributions derived from standard ground motion selection practices. The conversion process applies these conditional distributions for each rupture scenario to progressively transform the original fragility from one IM representation to another. While computationally more demanding than earlier methods, this methodology avoids oversimplifying assumptions and exploits comprehensive hazard information to achieve more accurate conversions.

As a result, an original fragility function defined in terms of IM_1 is transformed to a converted fragility in terms of IM_2 by using Equation (4). For a given value of $IM_2=im_2$, and for each value of IM_1 considered as part of the integral, Equations (6), (7), and (8) are applied for each rupture scenario to compute the conditional distribution $f_{IM1|IM2,Rup}$

using Equation (5). Integrating this with the original fragility function $P[DS|IM_1]$ gives the complete distribution $P[DS|IM_2]$.

$$f(IM1|IM2,Rup)\sim N(\mu(\ln IM1|\ln IM2,Rup),\ \sigma(\ln IM1|\ln IM2,Rup)) \quad (5)$$

$$\mu(lnIM1|lnIM2,Rup) = \mu(\ln IM1|Rup) + \rho(\ln IM1,\ln IM2)\,\sigma(\ln IM1) \quad (6)$$

$$\epsilon(\ln IM2|Rup) = \ln im2 - \mu(\ln IM2|Rup)\,\sigma(\ln IM2|Rup) \quad (7)$$

$$\sigma(\ln IM1|\ln IM2,Rup2) = \sigma(\ln IM1|Rup2)\sqrt{1-\rho(\ln IM1,\ln IM2)^2} \quad (8)$$

where $\mu(\ln IM1|Rup)$ and $\sigma(\ln IM1|Rup)$ are the mean and standard deviation of IM_1 using a single GMM and rupture parameters collectively *Rup*, $\rho(\ln IM1,\ln IM2)$ is the correlation coefficient between the two IMs and is typically assumed as independent of *Rup* parameters (Aristeidou et al., 2024; Baker & Bradley, 2017). The epsilon term, $\epsilon(\ln IM2|Rup)$, represents the number of standard deviations above or below the mean GMM prediction of IM_2=im_2.

EXTENSION TO VULNERABILITY MODELLING

Existing conversion research has primarily addressed fragility functions describing damage state probabilities, yet comprehensive seismic risk assessment fundamentally depends on vulnerability functions characterising economic losses and other consequences. While fragility functions employ lognormal parametrisations, vulnerability functions rely on discrete distributions relating expected losses to ground motion intensity. Given that risk models frequently operate directly with vulnerability metrics rather than fragility, extending the total probability conversion methodology to vulnerability functions proves essential. This paper applies and tests this extension, adapting the previously described framework to accommodate vulnerability functions' discrete loss characterisations: $E[L|IM]$. The Equation (4) is extended to provide:

$$E(L|IM2) = \int_{IM1}\int_{Rup} E(L|IM1)\,f(IM1|IM2,Rup)\,f(Rup|IM2) \quad (9)$$

where the $E[L|IM_1]$ is the original vulnerability function and $E[L|IM_2]$ is the converted, with all other terms being the same as before.

ANALYSIS

Methodologies

The following methodologies were used to perform conversions for fragility/vulnerability functions from on original IM_1 to a new IM_2:

- Method 1 is the total probability approach outlined in the previous section. It uses the full disaggregation information obtained from OpenQuake defined in terms of

occurrence and the correlation model of Aristeidou et al. (2024), hence is termed the "exact" approach using Equation (4), given its probabilistic basis and scrutiny with respect to hazard information;
- Method 2 uses enough rupture scenarios so that 50% of the hazard is accounted for;
- Method 3 uses the mean *M*, *R* and GMM scenario from the disaggregation;
- Method 4 uses the modal *M*, *R* and GMM scenario from the disaggregation;

Overview of the case study

Case studies employing nonlinear response history analysis generated fragility functions across multiple IM definitions, including peak absolute quantities like PGA and PGV, spectral accelerations at several periods, *Sa*(0.5s), *Sa*(1s), *Sa*(1.5s), *Sa*(2s), filtered incremental velocity at several periods, *FIV*3(0.5s), *FIV*3(1s), *FIV*3(1.5s), *FIV*3(2s), two alterative definitions of average spectral acceleration as defined in Shahnazaryan and O'Reilly (2024) at several periods, Sa_{avg2}(0.5s), Sa_{avg2}(1s), Sa_{avg2}(1.5s), Sa_{avg2}(2s), and Sa_{avg3}(0.5s), Sa_{avg3}(1s), Sa_{avg3}(1.5s), Sa_{avg3}(2s). Each fragility function defined in terms of an original IM was converted to a target IM and compared against reference functions derived directly using the reference equivalent for the target IM. The analysis encompassed numerous combinations across multiple structural models, damage states, and conversion methodologies. Comparisons were conducted quantitatively through fitted lognormal parameters. The Hellinger distance metric (Hellinger, 1909) was used (Equation (10)), quantifying similarity between original converted fragility functions with values ranging from 0 (identical) to 1 (completely dissimilar) making it a useful metric for understanding how the overall similarity between original and converted fragility functions can be interpreted for all cases analysed.

$$H\ F\left(IM\right),\ F\left(IM\right) = \sqrt{1 - \sqrt{\frac{2\beta_1\beta_2}{\beta_1^2 + \beta_2^2}}\exp\left(-\frac{1}{4}\frac{\left(\mu_1 - \mu_2\right)^2}{\beta_1^2 + \beta_2^2}\right)} \quad (10)$$

Numerical models and analysis

The case studies were represented through four SDOF systems. The systems were modelled using OpenSees (McKenna et al., 2010; Zhu et al., 2018) and the backbone curves for the SDOFs are depicted in Figure 1. Models (1) to (3) are described through a uniaxial bilinear *Hysteretic* material with pinching factors of 0.8 and 0.5 for strain and stress, respectively, during reloading. Model (3) accounted for damage based on energy dissipation, while Model (4) used a uniaxial *Pinching4* material, including damage accumulation as a function of energy dissipation. A damping of 5% was applied using tangent stiffness proportional model. Five damage states (DS) were assigned to each of the systems, where DS1 defines the initiation of damage and is set at the 75% of yield displacement, and DS4 corresponds to significant damage and matches the point of fracturing, while intermediate damage states are evenly spaced between DS1 and DS4. Finally, complete damage (DS5) is assumed to occur at the system's ultimate displacement capacity, where base shear coefficient is zero. Based on the defined DSs, a damage-to-loss model, otherwise called a consequence model was defined for the systems from O'Reilly and Shahnazaryan (2024). The model is described through discrete damage to loss conversion points. Equation (11) represents the vulnerability function given as expected loss ratio versus intensity.

$$E\ L\square T\square|IM\square = i\square\square E\ L|D\ S\square i\square\square P\ D\ S\square i\square|IM\square\square \quad (11)$$

where $E[L|DS_i]$ is the loss corresponding to DS i, and $P[DS_i|IM]$ is the fragility function corresponding to DS i.

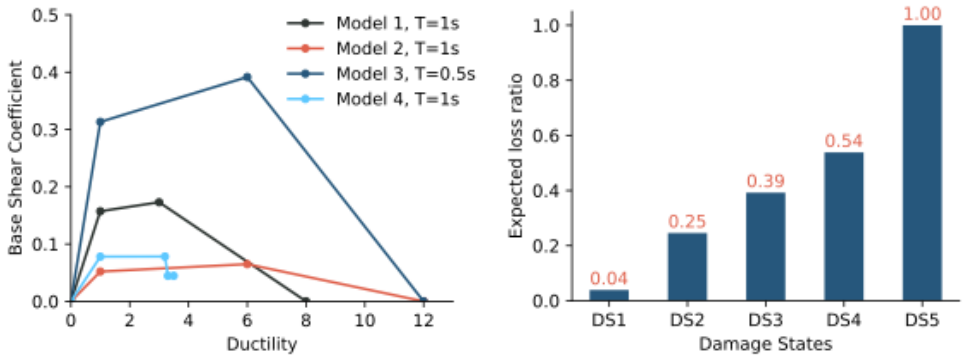

Figure 1. (left) Backbone curves of the SDOFs used, and (right) damage-to-loss model

PSHA was performed using the OpenQuake engine (Pagani et al., 2014) for the site of L'Aquila, Italy, using the Stucchi et al. (2004) source model. The hazard curves for the IMs of interest are given in Figure 2. A set of 40 ground motion records (single component) was selected using the NGA West-2 database (Ancheta et al., 2014) for each IM and POE level. The conditional spectrum was employed using the Djura Record Selector (https://app.djura.it) (Shahnazaryan et al., 2025). Figure 2 also demonstrates the hazard consistency checks for the ground motion set selected for a sample case of *IM*=*Sa*(1.0s), where a good agreement was observed across all IMs of interest.

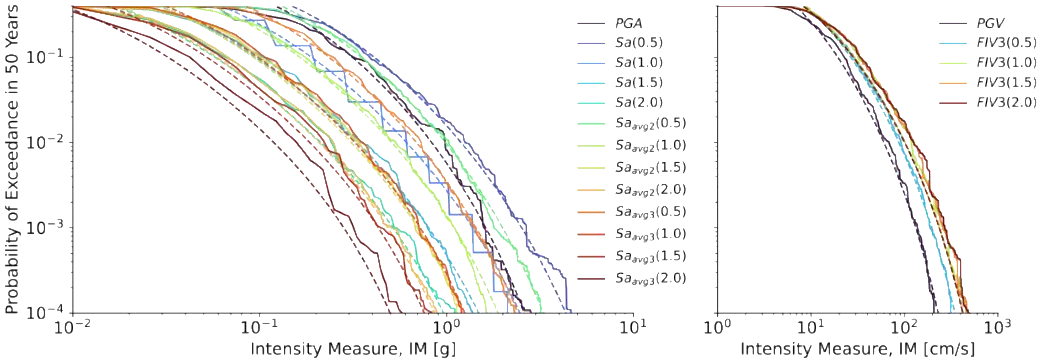

Figure 2. Hazard curves for each IM considered (dashed lines) with the hazard consistency checks (solid lines) for the selected ground motion record sets conditioned on IM=Sa(1s).

Multiple stripe analysis (MSA) was performed using the ground motion sets on each of the SDOF systems. For each SDOF system, fragility functions were developed at each DS and ground motion record set. Fragility functions were developed by counting the number of exceedances of system's DS threshold at each IM level, and fitting lognormal distribution to the data via maximum likelihood method. Finally, vulnerability functions were derived using Equation (11).

MODEL CONVERSION RESULTS

Fragility function comparisons

Figure 3 presents fragility function conversions for a single SDOF model across different DS and IM pairs. The plot grid is organised with the original IM_1 on the vertical axis and the converted IM_2 on the horizontal axis, which means that the first row, first column (starting from the bottom left) gives the case of an IM_1=Sa(2s) fragility function converted to IM_2=PGA. All methods performed particularly well when converting from longer-period $Sa(T)$-based IMs to shorter periods (e.g., IM_1=Sa(1s) to IM_2=Sa(0.5s)). Method 1's consideration of all possible hazard scenarios offered no clear advantage over Method 2, which achieved comparable accuracy across all variations.

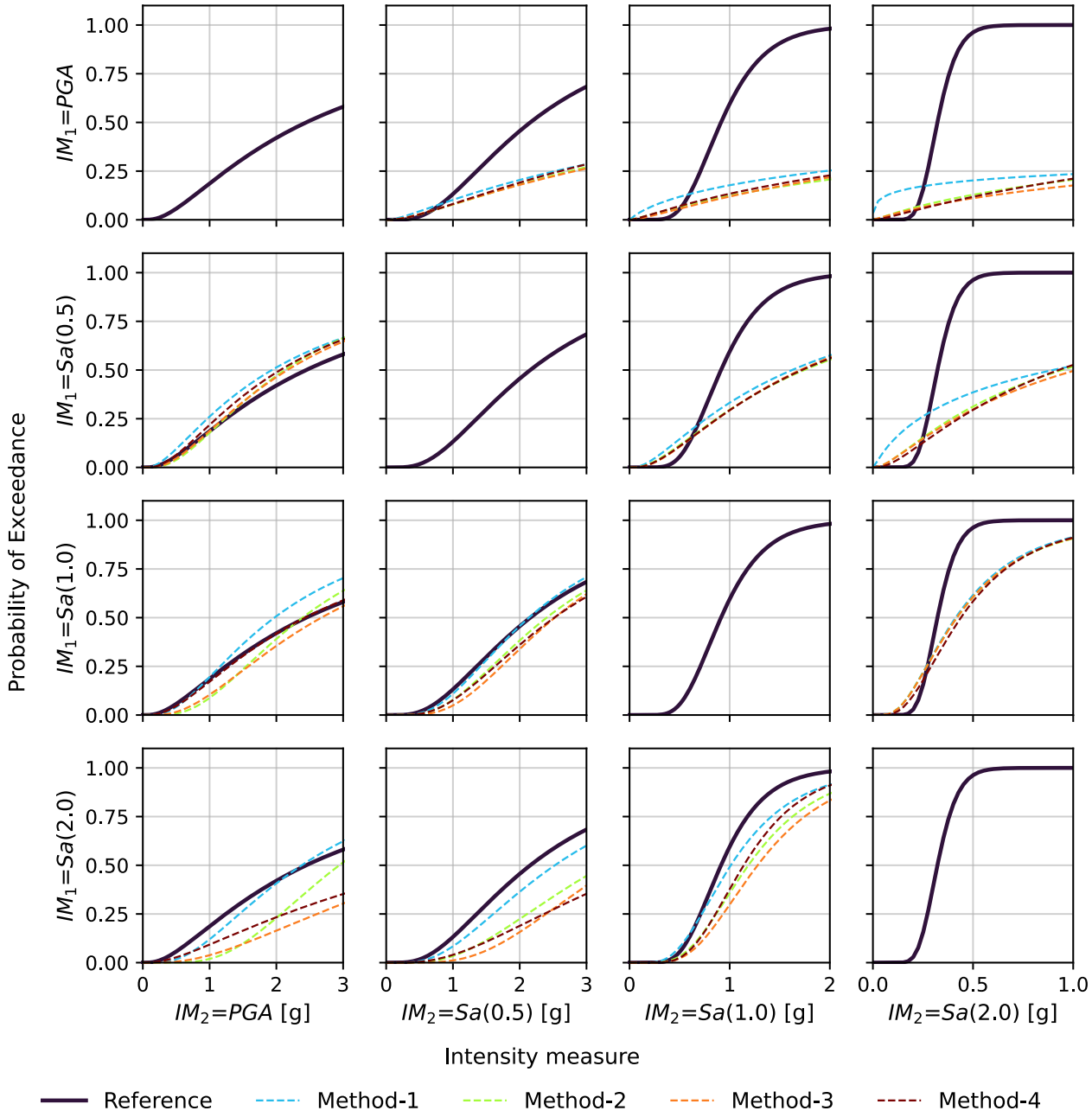

Figure 3. Comparison of reference and converted fragility functions for Model 1 at DS5 using traditional IMs such as PGA and Sa(T)

Figure 4 examines next-generation IMs such as $FIV3(T)$ and $Sa_{avg}(T)$, alongside PGV. The trends mirrored those of $Sa(T)$-based conversions. Again, all methods performed

relatively well, though this accuracy gap narrowed considerably for next-generation IMs due to their improved efficiency and lower dispersion in characterising structural damage. Additionally, there are still persistent bad conversions from low to high periods. This pattern held across all tested structures at each damage state. The findings align with Suzuki and Iervolino (2020) on spectral acceleration conversions. Converting from shorter to longer period worked well, but the reverse direction performed poorly. The conditional distribution becomes too broad and poorly constrained, pushing conversions into extrapolation regions where scalar IMs fail to capture actual structural response. Methods 3–5 appeared better in these cases, but this was misleading as constant dispersion assumptions simply limited how badly they could perform, masking low absolute accuracy. Suzuki and Iervolino (2020) addressed this by building vector-valued fragility surfaces using a hybrid linear–logistic model before conversion, highlighting the need for careful validation when converting to longer vibration periods.

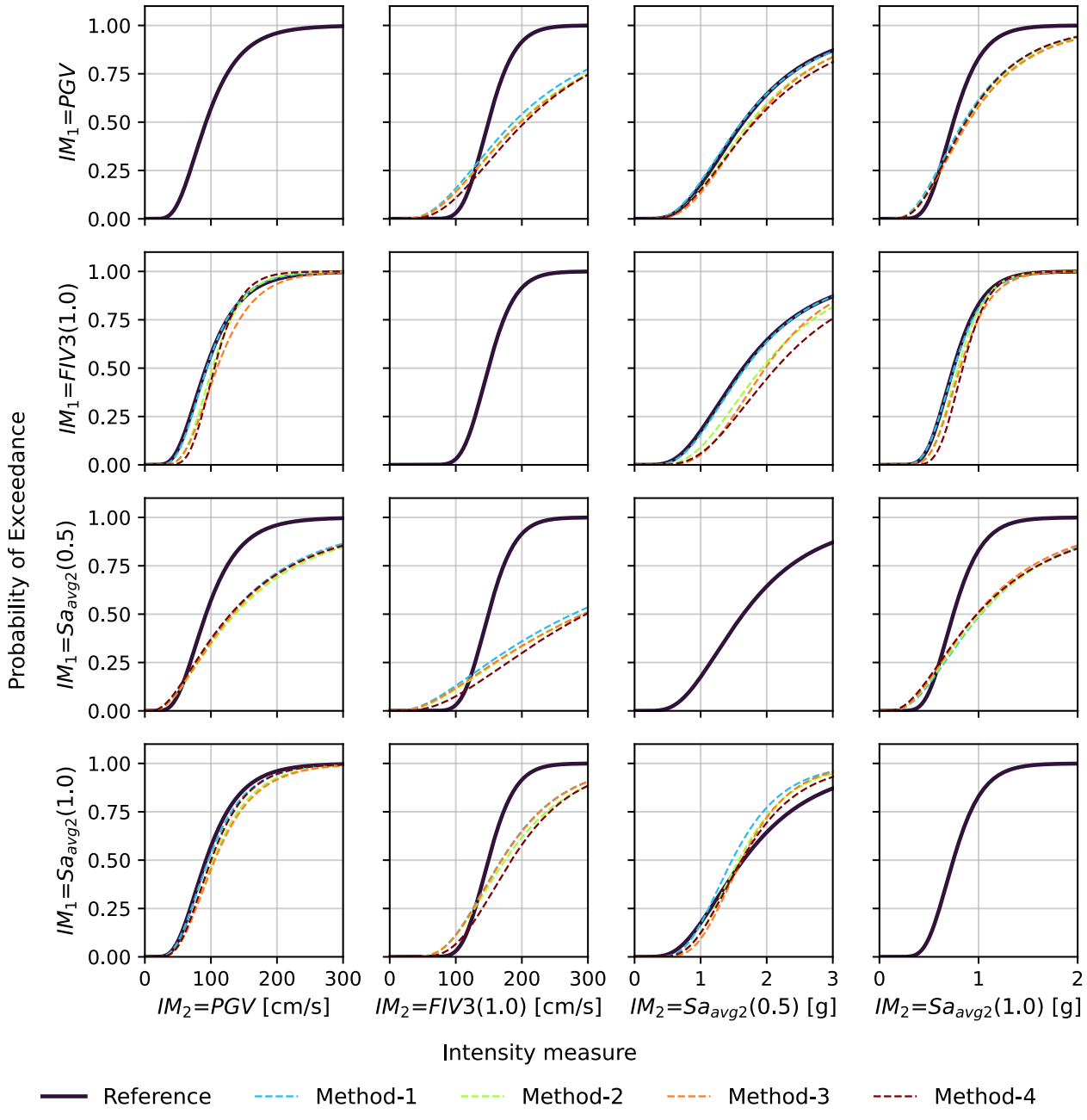

Figure 4. Comparison of reference and converted fragility functions for Model 1 at DS5 using next-generation IMs such as FIV3 and $Sa_{avg}(T)$

To gauge the conversion accuracy across all IMs, the Hellinger distance described in Equation (10) was used. These are plotted in Figure 5 as the average value across each DS and methods presented, and for all IM combinations considered. The colour red indicates a case where the conversion matched poorly to the reference fragility function, and green indicates a good conversion. *PGV* converts readily regardless of method, whereas *PGA* converts poorly. This reflects well-known efficiency and sufficiency limitations of *PGA*, and the loss of information when characterising fragility functions in terms of *PGA* cannot be recovered when converting to a more effective IM. Hence, it is strongly recommended not to develop fragility functions for regional applications in terms of *PGA*. Conversions among *FIV*3(*T*) variants are consistently excellent, which aligns with findings by Aristeidou et al. (2024) showing high self-correlation and period-independence for this IM. The results confirm that switching between *FIV*3(*T*) definitions is straightforward with all methods. It also can be seen that when converting from IM_1=*FIV*3(*T*) to any other IM_2 type works very well, regardless of the conversion method adopted. In contrast to *PGA*, it is recommended to develop fragility functions in terms of *FIV*3(*T*) since it offers excellent conversion flexibility and has been shown to be a very efficient and sufficient IM in many different contexts (Aristeidou & O'Reilly, 2024, 2026; Dávalos & Miranda, 2020, 2021). Its period-independence allows a single value (e.g., *T*=1s) to serve all structural typologies with minimal accuracy loss.

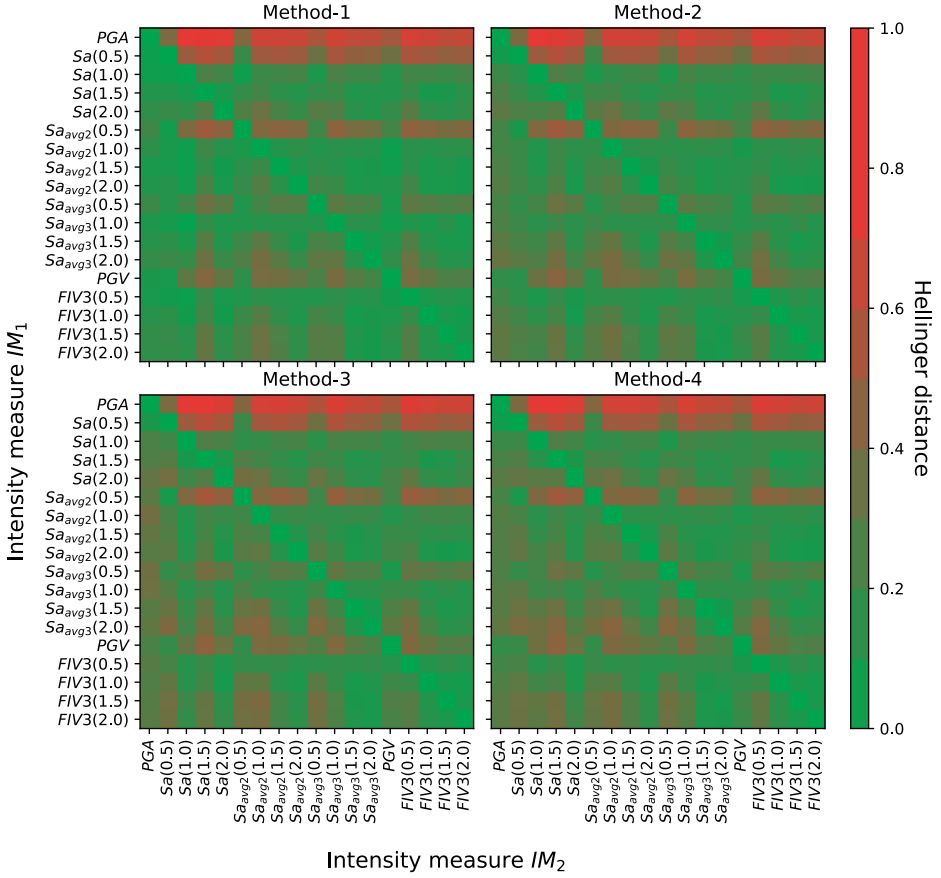

Figure 5. Hellinger distances between the reference and the converted fragility functions for Model 1 considering all methodologies outlined

Vulnerability function comparisons

While the previous section focused on converting fragility functions between different IMs, this section extends the analysis to vulnerability functions. Although fragility

functions underpin seismic risk models, vulnerability functions are more commonly used as the final output for assessing consequences such as monetary losses. The fragility function conversion was performed using Equation (4), following analogous assumptions regarding hazard and conditional dependence. Reference vulnerability functions were derived from the corresponding original fragility functions via Equation (11). Figure 6 presents the results, analogous to Figure 4. All methods yield very similar outcomes, suggesting that a simplified treatment of seismic hazard is generally sufficient. Overall, vulnerability function conversion performs well across different IMs, particularly at lower, more frequent intensity levels. To quantify the impact on risk metrics, average annual loss (AAL) was computed by integrating each vulnerability function with the seismic hazard. Figure 7 shows the resulting AAL differences relative to the reference vulnerability function.

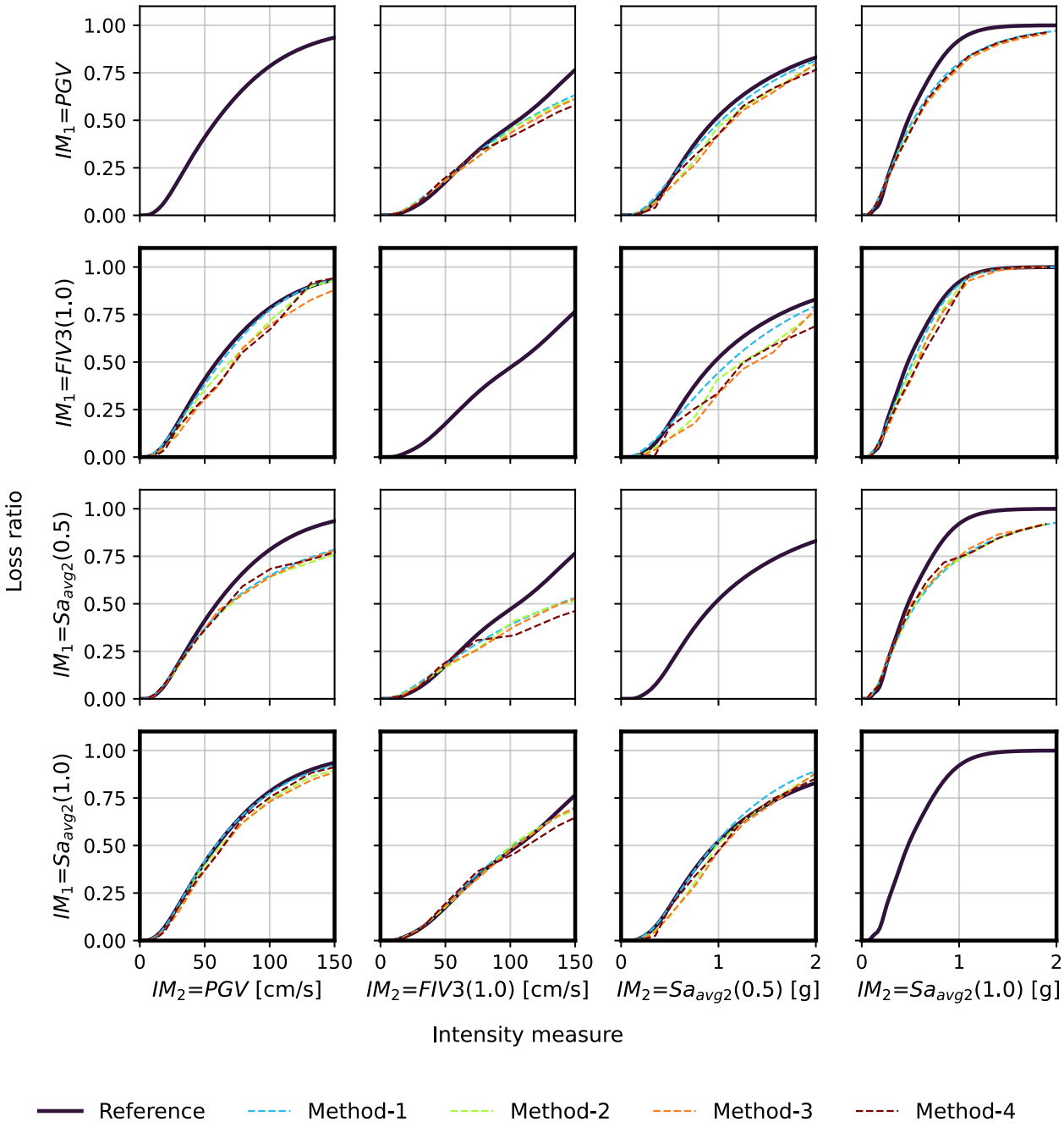

Figure 6. Comparison of reference and converted vulnerability functions for Model 1 using next-generation IMs such as FIV3, and $Sa_{avg}(T)$

Many trends present in fragility function conversion comparisons persist, and *PGA* again stands out. While previous results showed that converting other IMs to *PGA* produced good agreement at the fragility level, Figure 7 demonstrates that this leads to a substantial overestimation of AAL. This is attributed to the higher uncertainty associated with *PGA*, which inflates expected losses and, when integrated with hazard, results in biased AAL estimates. Consequently, harmonizing models in terms of *PGA* may appear convenient but proves problematic when extended to loss-based metrics. In contrast, *FIV*3(*T*) continues to perform well both when converting from or when converting to in all cases. Similarly, using $Sa_{avg}(T)$ as the original IM yields reliable conversions, further supporting the adoption of next-generation IMs in vulnerability modelling. Overall, vulnerability function conversions appear less susceptible to systematic errors that fragility function conversions, suggesting that risk modelers may benefit from focusing conversion efforts at the vulnerability level rather than at the fragility level, as has been common in the literature.

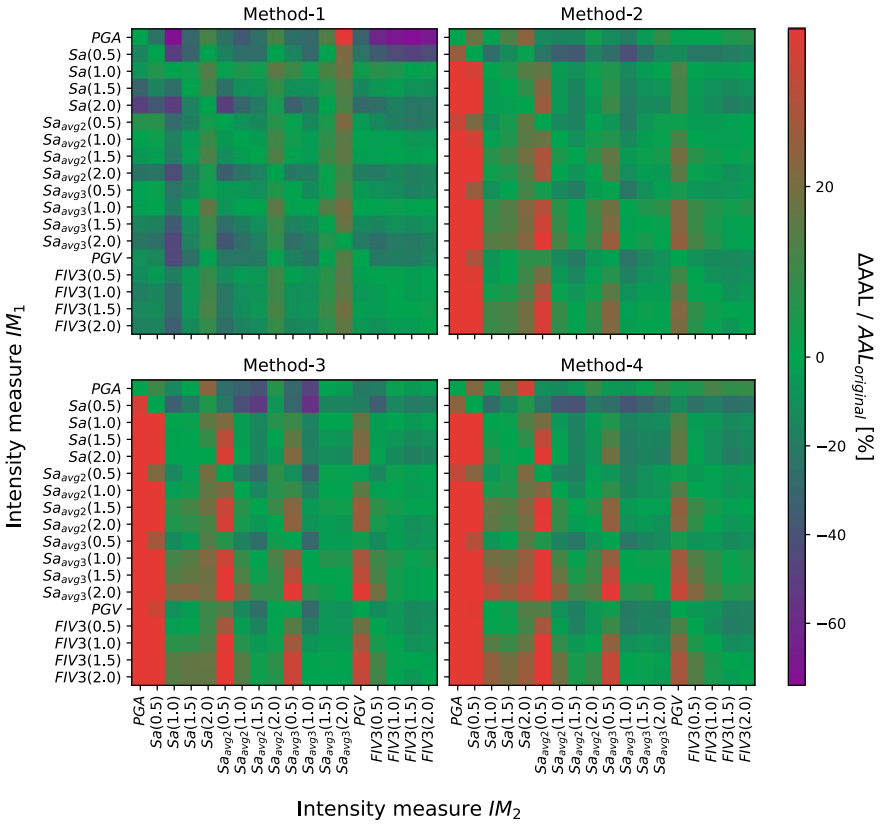

Figure 7. AAL ratio for vulnerability function conversions for Model 1

Site dependence is another key limitation worth addressing in future work. All fragility and vulnerability functions derived here apply to a single site, and their transferability to regions with different tectonic settings remains an open question, especially given how seismic hazard information enters the conversion equations. This issue is not unique to the present study; existing fragility and vulnerability models are similarly affected, though rarely acknowledged as such. The degree of site independence depends largely on the choice of IM. Kohrangi et al. (2017) showed that conventional IMs such as *Sa*(*T*) exhibit site dependence, while next-generation candidates like $Sa_{avg}(T)$ may not, offering considerably more flexibility. Should this hold for the conversions developed here, the consequences would be meaningful on two fronts: analysts would be steered toward more efficient IMs, improving loss estimation

accuracy, and greater freedom would exist when selecting between models for a given application, since more efficient IMs have already been shown to convert more reliably

SUMMARY AND CONCLUSIONS

There is no simple solution to reconciling fragility or vulnerability models defined using different intensity measures (IM)s. A common practice has been to adopt a single IM, most often peak ground acceleration (PGA), but efficiency and sufficiency considerations and the results of this show that PGA is a poor choice. Its use restricts model conversion and can significantly overestimate losses. In contrast, next-generation IMs such as average spectral acceleration and filtered incremental velocity (*FIV*3(*T*)) offer similar practicality while avoiding many of the biases associated with PGA, supporting their use in future modeling efforts. All methods require computation implementation, and supporting tools are provided in the accompanying repository (https://github.com/djura-risk-data-engineering/fragility-vulnerability-im-conversion).

The proposed methodologies along with available methodologies were applied on several case study systems. The other conclusions are as follows:

- For period-dependent IMs, conversion from longer to shorter periods is generally effective, but not vice versa;
- Although conversions to PGA can be accurate at the fragility level, extending them to vulnerability leads to systematic overestimation of losses and is therefore discouraged;
- The next-generation IM *FIV*3(*T*) shows strong promise due to its efficiency, site sufficiency, and ease of conversion to other IMs.

Finally, while the work focuses on converting models to a common IM, emerging cross-IM spatial correlation models may reduce the need for such conversions in future analyses, at the cost of increased computation effort.

ACKNOWLEDGMENTS

The work presented here has been developed within the framework of the "Sensor-driven statistical tools to evaluate risks and manage safety in the built environment" (SONATA) project, which is a Starting Grant awarded by the Italian Science Fund (Fondo Italiano per la Scienza) at IUSS Pavia under grant number FIS2023-03215.

REFERENCES

Abarca, A., Monteiro, R., & O'Reilly, G. J. (2022). Simplified methodology for indirect loss–based prioritization in roadway bridge network risk assessment. *International Journal of Disaster Risk Reduction*, *74*, 102948. https://doi.org/10.1016/j.ijdrr.2022.102948

Abarca, A., Monteiro, R., & O'Reilly, G. J. (2025). Seismic risk prioritisation schemes for reinforced concrete bridge portfolios. *Structure and Infrastructure Engineering*, *21*(1), 49–69. https://doi.org/10.1080/15732479.2023.2187424

Ancheta, T. D., Darragh, R. B., Stewart, J. P., Seyhan, E., Silva, W. J., Chiou, B. S. J., Wooddell, K. E., Graves, R. W., Kottke, A. R., Boore, D. M., Kishida, T., & Donahue, J. L. (2014). NGA-West2 database. *Earthquake Spectra*, *30*(3), 989–1005. https://doi.org/10.1193/070913EQS197M

Aristeidou, S., & O'Reilly, G. J. (2024). Exploring the Use of Orientation-Independent Inelastic

Spectral Displacements in the Seismic Assessment of Bridges. *Journal of Earthquake Engineering*, *28*(12), 3515–3538. https://doi.org/10.1080/13632469.2024.2343067

Aristeidou, S., & O'Reilly, G. J. (2026). Implications of conventional and next-generation intensity measure-based ground motion record selection for risk assessment of bridges. *Under Review*.

Aristeidou, S., Shahnazaryan, D., & O'Reilly, G. J. (2024). Correlation models for next-generation amplitude and cumulative intensity measures using artificial neural networks. *Earthquake Spectra*. https://doi.org/10.1177/87552930241270563

Baker, J. W., & Bradley, B. A. (2017). Intensity Measure Correlations Observed in the NGA-West2 Database, and Dependence of Correlations on Rupture and Site Parameters. *Earthquake Spectra*, *33*(1), 145–156. https://doi.org/10.1193/060716eqs095m

Bradley, B. A. (2010). A generalized conditional intensity measure approach and holistic ground-motion selection. *Earthquake Engineering & Structural Dynamics*, *39*(12), 1321–1342. https://doi.org/10.1002/eqe.995

Bradley, B. A. (2012). The seismic demand hazard and importance of the conditioning intensity measure. *Earthquake Engineering & Structural Dynamics*, *41*(11), 1417–1437. https://doi.org/10.1002/eqe.2221

Dávalos, H., & Miranda, E. (2019). Filtered incremental velocity: A novel approach in intensity measures for seismic collapse estimation. *Earthquake Engineering & Structural Dynamics*, *48*(12), 1384–1405. https://doi.org/10.1002/eqe.3205

Dávalos, H., & Miranda, E. (2020). Evaluation of FIV3 as an Intensity Measure for Collapse Estimation of Moment-Resisting Frame Buildings. *Journal of Structural Engineering*, *146*(10). https://doi.org/10.1061/(ASCE)ST.1943-541X.0002781

Dávalos, H., & Miranda, E. (2021). Robustness evaluation of fiv3 using near-fault pulse-like ground motions. *Engineering Structures*, *230*, 111694. https://doi.org/10.1016/j.engstruct.2020.111694

Eads, L., Miranda, E., & Lignos, D. G. (2015). Average spectral acceleration as an intensity measure for collapse risk assessment. *Earthquake Engineering & Structural Dynamics*, *44*(12), 2057–2073. https://doi.org/10.1002/eqe.2575

Esposito, S., Iervolino, I., D'Onofrio, A., Santo, A., Cavalieri, F., & Franchin, P. (2015). Simulation-Based Seismic Risk Assessment of Gas Distribution Networks. *Computer-Aided Civil and Infrastructure Engineering*, *30*(7), 508–523. https://doi.org/10.1111/mice.12105

Fox, M. J., Stafford, P. J., & Sullivan, T. J. (2016). Seismic hazard disaggregation in performance-based earthquake engineering: occurrence or exceedance? *Earthquake Engineering & Structural Dynamics*, *45*(5), 835–842. https://doi.org/10.1002/eqe.2675

Franchin, P., & Cavalieri, F. (2015). Probabilistic Assessment of Civil Infrastructure Resilience to Earthquakes. *Computer-Aided Civil and Infrastructure Engineering*, *30*(7), 583–600. https://doi.org/10.1111/mice.12092

Hellinger, E. (1909). Neue Begründung der Theorie quadratischer Formen von unendlichvielen Veränderlichen. *Journal Für Die Reine Und Angewandte Mathematik*, *1909*(136), 210–271. https://doi.org/10.1515/crll.1909.136.210

Heresi, P., & Miranda, E. (2022). Structure-to-structure damage correlation for scenario-based regional seismic risk assessment. *Structural Safety*, *95*, 102155. https://doi.org/10.1016/j.strusafe.2021.102155

Kazantzi, A. K., & Vamvatsikos, D. (2015). Intensity measure selection for vulnerability studies of building classes. *Earthquake Engineering & Structural Dynamics*, *44*(15), 2677–2694. https://doi.org/10.1002/eqe.2603

Kohrangi, M., Vamvatsikos, D., & Bazzurro, P. (2017). Site dependence and record selection schemes for building fragility and regional loss assessment. *Earthquake Engineering and Structural Dynamics*, *46*(10), 1625–1643. https://doi.org/10.1002/eqe.2873

Lin, T., Haselton, C. B., & Baker, J. W. (2013). Conditional spectrum-based ground motion selection. Part I: Hazard consistency for risk-based assessments. *Earthquake Engineering & Structural Dynamics*, *42*(12), 1847–1865. https://doi.org/10.1002/eqe.2301

McKenna, F., Scott, M. H., & Fenves, G. L. (2010). Nonlinear Finite-Element Analysis Software Architecture Using Object Composition. *Journal of Computing in Civil Engineering*, *24*(1), 95–107. https://doi.org/10.1061/(asce)cp.1943-5487.0000002

Mejia, T., & O'Reilly, G. J. (2026). Quantifying the Impacts of Incorporating Damage Correlation on Scenario-Based Regional Seismic Assessment. *Earthquake Engineering & Structural Dynamics*, *55*(1), 94–111. https://doi.org/10.1002/eqe.70069

Michel, C., Crowley, H., Hannewald, P., Lestuzzi, P., & Fäh, D. (2018). Deriving fragility functions from bilinearized capacity curves for earthquake scenario modelling using the conditional spectrum. *Bulletin of Earthquake Engineering*, *16*(10), 4639–4660. https://doi.org/10.1007/s10518-018-0371-3

Monteiro, V. A., & O'Reilly, G. J. (2026). A review of ground motion correlation modelling for regional seismic risk analysis. *Bulletin of Earthquake Engineering*. https://doi.org/10.1007/s10518-026-02377-0

O'Reilly, G. J., & Calvi, G. M. (2020). Quantifying seismic risk in structures via simplified demand–intensity models. *Bulletin of Earthquake Engineering*, *18*(5), 2003–2022. https://doi.org/10.1007/s10518-019-00776-0

O'Reilly, G. J., & Shahnazaryan, D. (2024). On the utility of story loss functions for regional seismic vulnerability modeling and risk assessment. *Earthquake Spectra*, *40*(3), 1933–1955. https://doi.org/10.1177/87552930241245940

Pagani, M., Monelli, D., Weatherill, G., Danciu, L., Crowley, H., Henshaw, P., Butler, L., Nastasi, M., Panzeri, L., Simionato, M., & Vigano, D. (2014). *OpenQuake Engine : An Open Hazard (and Risk) Software for the Global Earthquake Model*. *September*. https://doi.org/10.1785/0220130087

Shahnazaryan, D., & O'Reilly, G. J. (2024). Next-generation non-linear and collapse prediction models for short- to long-period systems via machine learning methods. *Engineering Structures*, *306*, 117801. https://doi.org/10.1016/j.engstruct.2024.117801

Shahnazaryan, D., O'Reilly, G. J., & Ozsarac, V. (2025). Djura Ground Motion Record Selector: A Software Solution For Earthquake Engineering. *COMPDYN 2025- 10th ECCOMAS Thematic Conference on Computational Methods in Structural Dynamics and Earthquake Engineering*.

Silva, V., Crowley, H., & Colombi, M. (2014). *Fragility Function Manager Tool* (pp. 385–402). https://doi.org/10.1007/978-94-007-7872-6_13

Stucchi, M., Albini, P., Mirto, M., & Rebez, A. (2004). Assessing the completeness of Italian historical earthquake data. *Annals of Geophysics*, *47*(2–3). https://doi.org/10.4401/ag-3330

Suzuki, A., & Iervolino, I. (2020). Intensity measure conversion of fragility curves. *Earthquake Engineering & Structural Dynamics*, *49*(6), 607–629. https://doi.org/10.1002/eqe.3256

Zhu, M., McKenna, F., & Scott, M. H. (2018). OpenSeesPy: Python library for the OpenSees finite element framework. *SoftwareX*, *7*, 6–11. https://doi.org/10.1016/j.softx.2017.10.009